Title

4EBP1/eIF4E and p70S6K/RPS6 axes play critical and distinct roles in hepatocarcinogenesis driven by AKT and N-Ras proto-oncogenes in mice

Journal

Hepatology, 61(1)

ISSN

0270-9139

Authors

Wang, Chunmei
Cigliano, Antonio
Jiang, Lijie
et al.

Publication Date

2015

DOI

10.1002/hep.27396

Peer reviewed

Published in final edited form as:
Hepatology. 2015 January ; 61(1): 200–213. doi:10.1002/hep.27396.

4EBP1/eIF4E and p70S6K/RPS6 Axes Play Critical and Distinct Roles in Hepatocarcinogenesis Driven by AKT and N-Ras Protooncogenes

Chunmei Wang[1], **Antonio Cigliano**[3], **Lijie Jiang**[1], **Xiaolei Li**[1,4], **Biao Fan**[1], **Maria G. Pilo**[3], **Yan Liu**[1], **Bing Gui**[1], **Marcella Sini**[3], **Jeffrey W. Smith**[5], **Frank Dombrowski**[3], **Diego F. Calvisi**[3], **Matthias Evert**[3], and **Xin Chen**[1,2]

[1]Department of Bioengineering and Therapeutic Sciences, University of California, San Francisco, CA

[2]Liver Center, University of California, San Francisco, CA

[3]Institute of Pathology, University of Greifswald, Greifswald, Germany

[4]Department of Hepatobiliary Surgery, Xijing Hospital, The Fourth Military Medical University, Xi'an, Shaanxi 710032, P. R. China

[5]Sanford-Burnham Medical Research Institute, La Jolla, CA

Abstract

Concomitant expression of activated forms of AKT and Ras in the mouse liver (AKT/Ras) leads to rapid tumor development via strong activation of the mTORC1 pathway. mTORC1 functions via regulating p70S6K/RPS6 and 4EBP1/eIF4E cascades. How these cascades contribute to hepatocarcinogenesis remains unknown. Here, we show that inhibition of RPS6 pathway via Rapamycin effectively suppressed, whereas blockade of the 4EBP1/eIF4E cascade by 4EBP1A4, an unphosphorylatable form of 4EBP1, significantly delayed, AKT/Ras induced hepatocarcinogenesis. Combined treatment with Rapamycin and 4EBP1A4 completely inhibited AKT/Ras hepatocarcinogenesis. This strong anti-neoplastic effect was successfully recapitulated by ablating *Raptor*, the major subunit of mTORC1, in AKT/Ras-overexpressing livers. Furthermore, we demonstrate that overexpression of eIF4E, the protooncogene whose activity is specifically inhibited by 4EBP1, resulted in HCC development in cooperation with activated Ras. Mechanistically, we identified the ENTPD5/AK1/CMPK1 axis and the mitochondrial biogenesis pathway as targets of the 4EBP1/eIF4E cascade in AKT/Ras and Ras/eIF4E livers as well as in human HCC cell lines and tissues.

Conclusions—Complete inhibition of mTORC1 is required to suppress liver cancer development induced by AKT and Ras protooncogenes in mice. The mTORC1 effectors, RPS6 and eIF4E, play distinct roles and are both necessary for AKT/Ras hepatocarcinogenesis. These

Contact Information: Xin Chen, UCSF, 513 Parnassus Ave., San Francisco, CA 94143, U.S.A. Tel: (415) 502-6526; Fax: (415) 502-4322; xin.chen@ucsf.edu; or Matthias Evert, Institut für Pathologie, Universitätsmedizin Greifswald, Friedrich-Löffler-Str. 23e, 17489 Greifswald, Germany. Tel: 0049 3834 865719; Fax: 0049 3834 865772; matthias.evert@uni-greifswald.de; or Diego F. Calvisi, Institut für Pathologie, Universitätsmedizin Greifswald, Friedrich-Löffler-Str. 23e, 17489 Greifswald, Germany. Tel: 0049 3834 865719; Fax: 0049 3834 865704; diego.calvisi@unigreifswald.de.

new findings might open the way for innovative therapies against human hepatocellular carcinoma.

Introduction

Hepatocellular carcinoma (HCC) is the most common type of liver cancer and the fourth leading cause of cancer death worldwide.[1] Treatment options for HCC are limited and generally ineffective: only a small percentage of HCC is diagnosed at an early stage and amenable to potential curative treatments such as surgical resection, liver transplantation, and radiofrequency ablation.[2–4] The only approved drug for the treatment of advanced HCC is Sorafenib, a multi-kinase inhibitor, whose overall efficacy in terms of patient's survival extension is, however, rather limited.[5] Thus, the development of novel therapeutic strategies against advanced HCC is mandatory. For this purpose, a deeper knowledge of the molecular mechanisms underlying hepatocarcinogenesis is necessary.[6,7]

One of the most frequently activated pathways in HCC is the PI3K/AKT/mTOR cascade,[8] which has been implicated in tumor initiation, progression, and metastasis.[9,10] Following PI3K (phosphoinositide 3-kinase) activation by receptor tyrosine kinases or G protein coupled receptors, AKT (v-akt murine thymoma viral oncogene homolog) is recruited to the membrane and phosphorylated.[9,10] In mouse hepatocytes, overexpression of an activated form of AKT (Myr-AKT) induces lipogenesis and hepatocyte proliferation, eventually leading to HCC development within six months.[11] AKT exerts many effects on target cells through its key downstream effector, the mTOR complex 1 (mTORC1).[10,12]

The mTORC1 axis is also frequently activated in human HCC.[13] Using mice with liver-specific deletion of *TSC1* and *Raptor* (regulatory associated protein of mTORC1, an essential mTORC1 component), a recent study showed that mTORC1 controls ketogenesis in mice in response to fasting and its modulation by ageing.[14] Moreover, chronic activation of mTORC1 in mice with liver-specific deletion of *TSC1* leads to hepatocarcinogenesis.[15]

The major regulators downstream of mTORC1 are 4EBP1 and p70S6K1/2.[16,17] 4EBP1 negatively regulates eIF4E, a key rate-limiting initiation factor for cap-dependent translation. Phosphorylation by mTORC1 leads to 4EBP1 dissociation from eIF4E, allowing translation initiation complex formation at the 5' end of mRNAs. 4EBP1/eIF4E mediated translational control has been shown to be the key downstream signal of mTORC1 in AKT-induced lymphomagenesis *in vivo*,[18] and a critical mediator of mTORC1-induced cell proliferation.[19] Moreover, 4EBP1/eIF4E has been found to be a major effector of the oncogenic activation of AKT and ERK signaling pathways in tumor cell lines and xenograft models.[20] p70S6K1/2 is another downstream effector of mTORC1. Once phosphorylated and activated by mTORC1, p70S6K1/2 in turn regulates 40S ribosomal protein S6 (RPS6) as well as other regulators of translation initiation.[21] Ablation of *RPS6* in mouse hepatocytes inhibits cell proliferation after partial hepatectomy.[22,23] Also, when all the five phosphorylatable serine residues of RPS6 are substituted by unphosphorylatable alanine, knock-in *RPS6*($P^{-/-}$) mice display cell growth defect.[24] Using *RPS6*($P^{-/-}$) mice, a previous study showed that loss of phosphorylation of RPS6 is dispensable for AKT-mediated lymphomagenesis.[18] Rapamycin, an allosteric partial inhibitor of mTORC1, and its

analogues (Rapalogs) have been tested clinically as anti-cancer agent in multiple tumor types.[25,26] However, Rapalogs only showed modest clinical efficacy, presumably due to their capacity to suppress phosphorylation of RPS6 but not 4EBP1.[27,28]

Concomitant activation of AKT/mTOR and Ras/MAPK cascades is frequently observed in human HCC.[13,29] To elucidate the molecular and biochemical crosstalk(s) between the two pathways, we generated a mouse model of liver cancer characterized by co-expression of activated forms of AKT and N-Ras.[30] In the current study, using genetic and pharmacological approaches, we systematically investigated the requirement of each of the two main mTORC1 downstream effectors, 4EBP1/eIF4E and p70S6K/RPS6, in AKT/Ras-induced hepatocarcinogenesis *in vivo*. Our data demonstrate that complete inhibition of mTORC1 is required to suppress hepatocarcinogenesis driven by N-Ras and AKT oncogenes in mice.

Materials and Methods

Hydrodynamic injection and mouse treatment

Wild-type FVB/N mice were obtained from Charles River (Wilmington, MA). *Raptor*$^{fl/+}$ mice were purchased from the Jackson Laboratory (Stock: 013188), and intercrossed to generate *Raptor*$^{fl/fl}$ mice.[14] Hydrodynamic injections were performed as described previously.[11, 30–32] To delete *Raptor* while co-expressing AKT and/or Ras, we injected high dose of pT3-Cre (20μg) with low dose of AKT (4μg) and/or Ras (4μg). To ensure that all oncogene expressing cells also express Cre which led to deletion of the targeted floxed alleles, we injected pT3-Cre (20μg) with HA tagged AKT (4μg) into *R26R-EYFP* mice. In the *R26R-EYFP mice*, Cre-mediated excision of the floxed termination sequence leads to constitutive *EYFP* expression.[33] Subsequent double immunofluorescence staining showed that all HA positive AKT expressing cells were also EYFP positive (Supplementary Fig. 1), supporting the notion that we were able to simultaneously delete the targeted floxed alleles while expressing the oncogene in the same set of hepatocytes. Rapamycin (6mg/kg/day) or vehicle was intraperitoneally administered for 7 or 11 weeks immediately after hydrodynamic injection. To block the 4EBP1/eIF4E cascade, high doses of 4EBP1A4 (20μg) with low doses of AKT (4μg) and/or Ras (4μg) were injected. To generate eIF4E and Ras/eIF4E mice, pT3-EF1α-HA-eIF4E (10μg) alone or with pT2CAGGS-NRasV12 (10 μg) was hydrodynamically injected into FVB/N mice. Wild-type (not injected) and mice injected with pT3-EF1α empty plasmid were used as controls; since no difference in any parameter analyzed between the two control groups was detected, the data were merged. Mice were housed, fed, and monitored in accordance with protocols approved by the committee for animal research at the University of California, San Francisco.

Detailed description of Materials and Methods is provided as Supplementary Material.

Results

Blocking of RPS6 Pathway via Rapamycin Effectively Inhibits AKT/Ras Hepatocarcinogenesis

We previously showed that Rapamycin administration for 3 weeks suppresses the activation of RPS6 but not p-4EBP1 in AKT/Ras mice.[34] To thoroughly investigate the contribution of p70S6K/RPS6 along AKT/Ras induced hepatocarcinogenesis, Rapamycin was administered daily for 7 weeks in AKT/Ras mice immediately after hydrodynamic injection (Supplementary Fig. 2A). In accordance with previous findings,[34] Rapamycin treatment efficiently blocked p-RPS6 expression in the liver of AKT/Ras mice without affecting p-4EBP1 levels (Fig. 6A). Suppression of p-RPS6 was paralleled by prevention of hepatocarcinogenesis in Rapamycin treated AKT/Ras mice. Indeed, none of the Rapamycin treated AKT/Ras mice developed palpable liver tumors 7 weeks post injection, whereas all vehicle treated AKT/Ras mice developed lethal burden of liver tumors (Fig. 1A, B).

Histologically, liver lesions from Rapamycin treated AKT/Ras mice consisted of few, small clusters of lipid-rich preneoplastic hepatocytes (Fig. 1C). Altered cells showed stable integration of the injected constructs (Fig. 1D), overexpression of p-AKT, and variable expression of p-ERK1/2 (positive cells shown) and p-mTOR (Fig. 1E). Equivalent, scattered clusters of preneoplastic hepatocytes but not tumor lesions were detected in 3 AKT/Ras mice in which Rapamycin was administered up to 11 weeks post-injection (data not shown), suggesting that continuous Rapamycin treatment might impede the appearance of frankly malignant tumors in AKT/Ras livers.

Altogether, these findings demonstrate that p70S6K/RPS6 is a critical downstream effector of mTORC1 and is required for AKT/Ras-driven hepatocarcinogenesis.

Inhibition of 4EBP1/eIF4E by 4EBP1A4 Delays AKT/Ras Induced Hepatocarcinogenesis

To investigate the contribution of the 4EBP1/eIF4E axis in AKT/Ras induced hepatocarcinogenesis, we overexpressed pT3-EF1α (pT3, empty vector, control), wild-type 4EBP1 (4EBP1WT), or 4EBP1A4, a mutant form of 4EBP1 that cannot be phosphorylated/inactivated by mTORC1,[18] along with AKT and N-Ras into the mouse liver via hydrodynamic injection (Supplementary Fig. 2B). Previous findings showed that 4EBP1A4 is able to efficiently block eIF4E mediated CAP-dependent translational initiation downstream of mTORC1.[18] Accordingly, we found that overexpression of 4EBP1A4, but not Rapamycin treatment, inhibited CAP-dependent translation in the AKT/Ras mouse liver tumor cell line (Supplementary Fig. 3). This cell line was used since it accurately recapitulates the molecular mechanisms responsible for AKT/Ras induced hepatocarcinogenesis.[34]

Seven weeks after hydrodynamic injection, none of the AKT/Ras/4EBP1A4 mice developed palpable liver masses (Fig. 2). In contrast, all mice from the AKT/Ras/pT3 and AKT/Ras/4EBP1WT cohorts developed lethal burden of liver tumors (Fig.2, Supplementary Fig. 4, 5). Grossly, only few very small nodules could be observed in the livers of AKT/Ras/4EBP1A4 mice whereas numerous large nodules equally developed in the livers of AKT/Ras/pT3 and AKT/Ras/4EBP1WT mice 7 weeks post injection (Fig. 2, Supplementary Fig. 4, 5).

Histologically, clusters of lipid-rich preneoplastic hepatocytes occupying ~40% of the liver parenchyma characterized AKT/Ras/4EBP1A4 mice at this time point (Fig. 2D). HA-tag and V5-tag were detected in the clear-cell preneoplastic hepatocytes, demonstrating the stable transfection of AKT (HA-tag) and 4EBP1A4 (V5-tag) in these cells (Fig. 2D). No frankly malignant lesions were detected.

Next, three AKT/Ras/4EBP1A4 mice were aged to determine whether liver tumor could eventually develop in these mice. Palpable liver masses were appreciable 21 weeks post injection (Fig. 3A and 2C). The liver of AKT/Ras/4EBP1A4 mice was occupied mainly by premalignant and HCA lesions, with some small HCC and ICC lesions (Fig. 3B). Tumors were proliferating, as indicated by Ki67 staining (Fig. 3C). Serial sections of liver tumors demonstrated the expression of the injected constructs, namely AKT (HA-tag) and 4EBP1A4 (V5-tag), indicating that these tumors developed in the presence of ectopically expressed 4EBP1A4 (Fig. 3C). Moreover, elevated immunoreactivity for p-AKT, p-ERK1/2 and p-mTOR was detected (Fig. 3D).

In summary, the data indicate that 4EBP1/eIF4E mediated CAP dependent translation initiation has a critical role along AKT/Ras hepatocarcinogenesis. Inhibition of 4EBP1/eIF4E significantly delays but cannot completely prevent liver tumor development in AKT/Ras mice.

Complete Inhibition of mTORC1 is Required to Suppress AKT/Ras Hepatocarcinogenesis

Although blocking of RPS6 or eIF4E resulted in a striking reduction of preneoplastic lesions and/or remarkable delay of tumor development, preneoplastic and/or neoplastic lesions were still observed following the two distinct treatments. Thus, we investigated whether complete suppression of mTORC1 by concomitant inhibition of RPS6 and eIF4E could completely abolish AKT/Ras hepatocarcinogenesis. For this purpose, mice co-injected with AKT, Ras and 4EBP1A4 were treated with Rapamycin (AKT/Ras/4EBP1A4/Rapa; n=5) or vehicle (AKT/Ras/4EBP1A4/Veh; n=3) for 7 weeks (Supplementary Fig. 2C). Macroscopically, no tumor nodules could be detected on the liver surface of AKT/Ras/4EBP1A4/Rapa mice (Fig. 4A and 4B). Histological examination revealed that the liver tissues from AKT/Ras/4EBP1A4/Rapa mice were nearly normal: only few isolated but never clusters of cells showed the lipid-rich features of AKT/Ras preneoplastic cells (Fig. 4C). The altered clear-cell hepatocytes were HA-positive, demonstrating the stable transfection with injected AKT (Fig. 4D). Of note, the few lipid-rich cells from AKT/Ras/4EBP1A4/Rapa mice show scarce or no activation of AKT, ERK, and mTOR proteins by immunohistochemistry (Fig. 4E), implying the suppression of these cascades in the residual preneoplastic cells. In contrast, AKT and ERK proteins were still activated in the small clusters of preneoplastic cells from Rapamycin treated AKT/Ras mice (AKT/Ras/Rapa; Fig. 1) and in preneoplastic lesions of AKT/Ras/4EBP1A4 injected mice (not shown). In addition, no difference in proliferative activity was detected in AKT/Ras/4EBP1A4/Rapa livers when compared with livers from mice injected only with empty vector (0.23 ± 0.2 vs. 0.25 ± 0.1, respectively; P = 0.9228; n=5 per each group).

To further validate the finding that complete inhibition of mTORC1 is required to fully suppress AKT/Ras induced liver tumor formation *in vivo*, we utilized *Raptor*$^{fl/fl}$ mice. We

co-injected AKT and Ras together with pT3-EF1α empty vector (AKT/Ras/pT3) or pT3-EF1α-Cre (AKT/Ras/Cre) in *Raptor*$^{fl/fl}$ mice (Supplementary Fig. 2D). We found that *Raptor*$^{fl/fl}$ mice injected with AKT/Ras/pT3 vector developed lethal burden of liver tumors within 6 to 8 weeks post injection. In striking contrast, *Raptor*$^{fl/fl}$ mice injected with AKT/Ras/Cre did not develop any preneoplastic or neoplastic lesion (Fig. 5A–C). Histologically, liver tumors from AKT/Ras/pT3 injected *Raptor*$^{fl/fl}$ mice were undistinguishable from those developed in wild type mice co-expressing AKT and Ras:[30] preneoplastic lesions and tumors occupied up to 90% of the liver parenchyma and tumor cells were highly proliferative (Fig. 5D). In contrast, liver tissues from AKT/Ras/Cre injected *Raptor*$^{fl/fl}$ mice were completely normal with no signs of preneoplastic or neoplastic lesions (Fig. 5E, upper panel). Only thorough histological investigation of the livers was able to detect very few single HA-positive clear-cell hepatocytes (Fig. 5E, lower panel). Noticeably, the observed effect was due to ablation of *Raptor* by Cre, and not the results of non-specific effects of Cre, as when AKT/Ras/Cre was injected into wild-type mice, lethal burden of liver tumors developed in these mice by 6 to 8 weeks post injection, similar to that observed in AKT/Ras injected mice (data not shown). To determine whether liver tumors might eventually develop over long term, AKT/Ras/Cre injected *Raptor*$^{fl/fl}$ mice were aged until 20 weeks post injection (n=3). None of the latter mice developed any preneoplastic or neoplastic lesion (Fig. 5A–C and data not shown).

Altogether, these studies demonstrate that AKT/Ras driven hepatocarcinogenesis depends on functional mTORC1 *in vivo*. Complete inhibition of mTORC1 is required to fully suppress hepatocarcinogenesis in this mouse model.

Inactivation of p70S6K/RPS6 and 4EBP1/eIF4E Axes Affects Proliferation but not Apoptosis of Preneoplastic Cells in AKT/Ras mice

Next, we investigated the cellular mechanisms responsible for inhibition of AKT/Ras-driven hepatocarcinogenesis following suppression of p70S6/RPS6 and/or 4EBP1/eiF4E cascades. For this purpose, we compared proliferative and apoptotic rates in preneoplastic lesions (or isolated preneoplastic cells) from the various models at the same time point (7 weeks post-injection; Supplementary Fig. 6). No significant differences in proliferation were detected when comparing wild-type livers with preneoplastic lesions from AKT/Ras/Cre injected *Raptor*$^{fl/fl}$ and AKT/Ras/4EBP1A4/Rapa mice, whereas a slightly higher proliferative activity was detected in AKT/Ras/Rapa mice. A progressive increase of proliferation occurred in preneoplastic lesions from AKT/Ras/4EBP1A4 mice. The highest proliferation index was observed in AKT/Ras/4EBP1WT and AKT/Ras mice. As concerns apoptosis, no significant differences were detected in cell death rate among the various mouse groups (Supplementary Fig. 6). These results suggest that suppression of the p70S6K/RPS6 and/or 4EBP1/eIF4E cascades is mainly associated with proliferation restraint in AKT/Ras mice.

p70S6K/RPS6 and 4EBP1/eIF4E Cascades Regulate Distinct Targets in AKT/Ras Liver Lesions

To further elucidate the molecular mechanisms of these pathways in AKT/Ras induced hepatocarcinogenesis, we assessed the effects of inhibiting the RPS6 or 4EBP1 axis in AKT/Ras livers at the molecular level by immunoblotting in wild-type, AKT/Ras, AKT/Ras/

Rapa, and AKT/Ras/4EBP1A4 liver tissues. Levels of phosphorylated/activated AKT were drastically reduced in the two experimental groups when compared with untreated AKT/Ras mice (Fig. 6A). Levels of phosphorylated/inactivated 4EBP1 were unmodified following Rapamycin treatment, whereas a strong induction of p-4EBP1 was detected in AKT/Ras/4EBP1A4 mice. The mechanism for the increased p-4EBP1 was not clear, but it was likely due to either increased phosphorylation of the endogenous 4EBP1 protein or cross-reaction of the anti-4EBP1 antibody with the injected 4EBP1A4 construct. Levels of eIF4E were unchanged in the two treated groups, whereas those of activated/phosphorylated eukaryotic initiation factor 4G (eIF4G), which binds eIF4E allowing the early steps of protein translation,[35] were completely abolished only in AKT/Ras/4EBP1A4 mice (Fig. 6A).

As mTORC1 is well characterized to exert its activity via regulating cell metabolism, we next investigated the effects of the treatments on metabolic pathways modulated by mTOR. SCD1 (involved in *de novo* lipogenesis) and PKM2 (glycolysis) were equally downregulated in the two treated groups. In contrast, some inducers of glycolysis, such as LDHA/C, ENTPD5 and its downstream effector AK1, were downregulated almost exclusively in AKT/Ras/4EBP1A4 mice. Importantly, LDHA/C downregulation occurred independent of c-Myc, since the latter was mainly downregulated following Rapamycin administration (Fig. 6B). Furthermore, although it has been demonstrated that ENTPD5 inhibits the endoplasmic reticulum (ER) stress pathway,[36,37] the levels of ER stress surrogate markers, including CHOP, BIP, and phosphorylated/activated PERK were not induced in AKT/Ras/4EBP1A4 mice (Fig. 6B). Since it has been recently found that 4EBP proteins negatively regulate mitochondrial activity and biogenesis,[38] we tested the levels of the master regulator of mitochondrial biogenesis, mitochondrial transcription factor A (TFAM). Of note, TFAM was only downregulated in AKT/Ras/4EBP1A4 mice (Fig. 6B). An additional established target of the 4EBP1/eIF4E axis, namely Cyclin D1, was downregulated only in AKT/Ras/4EBP1A4 mice. Finally, the importance of ENTPD5 in AKT/Ras-induced hepatocarcinogenesis was assessed by its siRNA-mediated silencing in the AKT/Ras cell line (Supplementary Fig. 7). Inhibition of ENTPD5 resulted in decrease of proliferation and induction of apoptosis in AKT/Ras cells when compared with control cells (Supplementary Fig. 7B, C). At the molecular level, AKT/Ras cells depleted of ENTPD5 did not show any relevant change in the levels of proteins involved in ER stress (BIP and p-PERK) or glycolysis (PKM2, LDHA/C, Hexokinase II or HXII, liver phosphofructokinase or PFKL, and aldolase A or ALDOA) (Supplementary Fig. 7A).

The present data indicate that p70S6K/RPS6 and 4EBP1/eIF4E cascades control different targets in AKT/Ras driven hepatocarcinogenesis.

Overexpression of eIF4E Cooperates with Ras to Induce Liver Tumor Development in Mice

Next, we sought to determine whether eIF4E, whose activity is inhibited by 4EBP1, is oncogenic in the mouse liver. For this purpose, the eIF4E gene tagged with HA was hydrodynamically transfected into wild-type mice. Neither preneoplastic nor neoplastic livers lesions developed in these mice up to 30 weeks post injection (Supplementary Figs. 8 and 9), although up to 10–15% of the hepatocytes showed the integration of the eIF4E construct (Supplementary Fig. 9), indicating that eIF4E alone does not suffice to

malignantly transform hepatocytes. Nevertheless, a significantly higher hepatocyte proliferation rate in eIF4E injected mice than in mice injected with empty plasmid was detected (1.22 ± 0.3 vs. 0.25 ± 0.1, respectively; n =5 per each group; $P < 0.0001$). At the molecular level, eIF4E livers showed a striking co-localization of HA with ENTPD5, CMPK1, and AK1, confirming that the latter axis is modulated by the 4EBP1/eIF4E cascade in the mouse liver. No immunoreactivity for p-ERK, p-AKT, p-mTOR, and p-RPS6 was detected in eIF4E-injected livers (Supplementary Fig. 9).

Next, we assessed whether eIF4E cooperates with the Ras/MAPK pathway, the other cascade not affected by Rapamycin treatment in AKT/Ras mice.[34] Our previous studies showed that overexpression of N-Ras alone via hydrodynamic injection did not lead to any liver morphologic alteration 30 weeks post-injection.[30] Similarly, co-expression of eIF4E and N-Ras did not result in hepatic histological alterations 19 weeks post injection (n=3; data not shown). However, multiple hepatocellular tumors, consisting of HCA and HCC, were detected in eIF4E/Ras mice 30 weeks post injection (n=6; Fig. 7A, B). As in eIF4E mice, hepatocytes from eIF4E/Ras mice expressing the HA-eIF4E protein also exhibited a strong immunolabeling for ENTPD5, CMPK1, and AK1 (Fig. 7C), while being negative for p-AKT, p-mTOR, and p-RPS6 staining (Fig. 7D). Of note, strong p-ERK staining was detected in preneoplastic and neoplastic lesions from eIF4E/Ras mice, indicating successful expression of the delivered Ras plasmid (Fig. 7D). Altogether, the present data indicate that eIF4E is not oncogenic *per se* in the mouse liver, but acts synergistically with N-Ras to induce hepatic tumor development independent of the AKT/p70S6K/RPS6 cascade.

4EBP1 Controls the ENTPD5 Axis in Human HCC Cell Lines and Tissues

Due to the novel finding about the link between 4EBP1 and ENTPD5 in AKT/Ras mice, we assessed whether the same applies for human HCC. For this purpose, we overexpressed either 4EBP1WT or 4EBP1A4 in the HLF human HCC cell line. Notably, overexpression of 4EBP14A and 4EBP1WT, at a lower extent, led to downregulation of ENTPD5 and its targets, AK1 and CMPK1, in HLF cells (Supplementary Fig. 10A). Consistent with the *in vivo* data, Rapamycin treatment had no effect on the expression of ENTPD5, AK1, or CMPK1 in HLF cells (Supplementary Fig. 10B). In addition, overexpression of 4EBP1WT and, mostly, 4EBP1A4 but not Rapamycin treatment resulted in downregulation of activated/phosphorylated eIF4G and TFAM proteins, in accordance with mouse data (Supplementary Fig. 10, Fig. 6). Furthermore, concomitant Rapamycin administration and 4EBP1A4 transient transfection resulted in a much more pronounced growth restraint than either treatment alone in HLF cells (Supplementary Fig. 11), confirming that the targets of the p70S6K/RPS6 and 4EBP1/eIF4E cascades are different in liver cancer.

Finally, we analyzed a collection of human HCC specimens (n=52) by immunohistochemistry for p-4EBP1, ENTPD5, AK1, and CMPK1. Stronger p-4EBP1, ENTPD5, AK1, and CMPK1 immunoreactivity when compared with non-tumorous surrounding counterparts was detected in 52%, 42.3%, 46.2%, and 55.8% of HCCs, respectively. Of note, 80% (20 of 25) of HCCs displaying increased p-4EBP1 immunoreactivity concomitantly showed up-regulation of ENTPD5, AK1, and CMPK1 (Fig. 8). No association between the staining patterns of p-4EBP1, ENTPD5, AK1, and

CMPK1 and clinicopathologic features of the patients, including etiology, presence of cirrhosis, α-fetoprotein levels, tumor grading, and survival length was detected (data not shown). Altogether, the present data indicate that 4EBP1/eIF4E controls the expression of ENTPD5 and its downstream effectors in human HCC.

Discussion

mTORC1 is the master regulator of a plethora of processes influencing cell proliferation and survival.[17] mTORC1 functions mainly via regulating p70S6K/RPS6 and 4EBP1/eIF4E cascades.[16,17] Of the two cascades, p70S6K/RPS6 is the best characterized. Once activated, the p70S6K/RPS6 axis triggers cell growth and proliferation by promoting protein and lipid synthesis, gene transcription, and cell metabolism.[21] Our current and previous studies demonstrate that Rapamycin specifically blocks p70S6K/RPS6 without affecting the 4EBP1/eIF4E cascade. Rapamycin treatment efficiently prevented AKT/Ras driven liver tumor development, suggesting that p70S6K/RPS6 is a critical downstream effector of mTORC1.

On the other hand, little is instead known about the 4EBP1/eIF4E cascade. In particular, the role of the 4EBP1/eIF4E pathway in cancer remains poorly understood. 4EBP1/eIF4E has been found to be a main effector of the AKT and ERK signaling pathways in *in vitro* and *in vivo* models.[20] As a consequence, it is not surprising that elevated levels of eIF4E have been described in multiple tumor types, including lung, bladder, colon, breast, prostate, cervix, ovary, and thyroid neoplasms[39,40] With regard to HCC, a recent investigation showed an increased eIF4E expression in tumor samples and a significant association between eIF4E levels and tumor recurrence.[41]

In the present study, we dissected for the first time the critical function of 4EBP1/eIF4E axis in the context of activated AKT/mTOR and Ras/MAPK cascades along hepatocarcinogenesis. Our data demonstrate that blocking eIF4E activity via the unphosphorylatable form of 4EBP1 (4EBP1A4) significantly delays both liver tumor development and progression induced by AKT and Ras oncogenes. Indeed, liver tumors were observed only after a long latency and consisted mainly of HCA and small HCC or ICC in AKT/Ras/4EBP1A4 mice. Nevertheless, despite the strong tumor suppressor activity, overexpression of 4EBP1A4 was unable to completely inhibit liver tumor development. This finding suggests that AKT/Ras driven hepatocarcinogenesis is able, at least in part, to overcome the deficiency of eIF4E and its related biologic effects.

At the cellular level, we found that inhibition of p70S6K/RPS6 and/or 4EBP1/eIF4E axes mainly affected proliferation rather than apoptosis of AKT/Ras preneoplastic cells, suggesting a direct correlation between proliferative activity of preneoplastic cells and propensity to tumor formation in this mouse model. Our data are in agreement with a previous study showing that everolimus, a Rapalog, efficiently inhibited chronic injury induced hepatocyte proliferation and DNA-damage induced liver tumor development in mice.[42] Altogether, these studies support the important role of mTORC1 in regulating hepatocyte proliferation, and suggest that suppression of p70S6K/RPS6 and/or 4EBP1/eIF4E axes may be helpful both to delay HCC development in patients at risk and to inhibit tumor recurrence.

Another major finding of the present study is the identification of novel downstream targets of the 4EBP1/eIF4E axis in the liver. Despite the assumption that eIF4E regulates translation at global level, mounting evidence suggest that it contributes to tumorigenesis by regulating a small set of proteins, such as Cyclin D1, VEGF, and c-Myc.[39,40] Here, we show that the ENTPD5/AK1/CMPK1 pathway is a major biochemical event downstream of eIF4E in mouse and human hepatocarcinogenesis. ENTPD5 is an endoplasmic reticulum (ER) UDPase that, together with AK1 and CMPK1, regulates a futile cycle which converts ATP into AMP, leading to compensatory increased aerobic glycolysis.[36,37] Thus, eIF4E might play a major role in promoting ATP consumption to satisfy the energetic and biosynthetic requirements of AKT/Ras cells. In addition, it has been found that ENTPD5 favours protein glycosylation and refolding, which protects tumor cells from protein overloading induced ER stress.[37] Surprisingly, we did not detect any sign of ER stress induction following inactivation of eIF4E by 4EBP1A4 overexpression both in AKT/Ras/4EBP1A4 mice and AKT/Ras cells. Similarly, ER stress and glycolysis proteins were not affected by ENTPD5 depletion in AKT/Ras cells. These findings suggest that ENTPD5 might play distinct roles that are context- or cell-type dependent. Although additional studies are needed to identify ENTPD5 targets in liver cancer, we have confirmed the strong connection between the 4EBP1/eIF4E and the ENTPD5/AK1/CMPK1 axes both in human HCC specimens and HLF cells, substantiating the important link between the two cascades in liver cancer.

Interestingly, we found that eIF4E controls also the final step of anaerobic glycolysis, since overexpression of 4EBP1A4 suppressed LDHA/C expression much more efficiently than Rapamycin in AKT/Ras mice. Furthermore, inactivation of eIF4E but not RPS6 resulted in the downregulation of the TFAM transcription factor, in accordance with the recent finding that the 4EBP1/eIF4E axis regulates mitochondrial activity and biogenesis.[38] Based on this body of data, it is tempting to speculate that the 4EBP1/eIF4E axis might be a central player in modulating aerobic and anaerobic glycolysis as well as mitochondrial dependent metabolisms.

Another major finding of the present study resides in the evaluation of the oncogenic potential of eIF4E in the mouse liver. We showed that eIF4E alone is not able to promote malignant transformation of murine hepatocytes, at least under our experimental conditions. Nevertheless, we found that eIF4E cooperates with activated N-Ras (whose overexpression *per se* is also unable to drive hepatocarcinogenesis[32]) to induce liver tumor development in the mouse. It is intriguing to note that both the Ras/MAPK and eIF4E cascades are not inhibited by Rapamycin in AKT/Ras mice.[34] Also, hepatocellular tumors eventually developing in eIF4E/Ras mice did not display the activation of the AKT/RPS6 cascade. Thus, we have identified a crosstalk between the Ras/MAPK and the eIF4E axes that is sufficient to drive hepatocarcinogenesis independent of the AKT/RPS6 pathway.

Rapamycin and Rapalogs, such as everilomus, have been tested clinically for HCC treatment and prevention. However, it has been recently reported that everolimus failed the Phase III trial for the treatment of advanced HCC (http://clinicaltrials.gov/ct2/show/NCT01035229?term=EVOLVE-1&rank=1), suggesting that partial inhibition of the mTORC1 cascade has very limited therapeutic efficacy in the treatment of liver cancer. Our current data strongly support the use of drugs which efficiently inhibit both p70S6K/RPS6 and 4EBP1/eIF4E

cascades. Importantly, inhibition of eIF4E via 4E2RCat, a compound isolated from a high throughput screening of molecules that inhibit the interaction between eIF4E and eIF4G, has shown encouraging anti-neoplastic effects.[43,44] Combinatorial administration of 4E2RCat (or similar drugs) and Rapamycin might represent an innovative approach for the treatment of cancers with elevated mTORC1 activity.

Supplementary Material

Refer to Web version on PubMed Central for supplementary material.

Acknowledgments

Grant Support:

This work was supported by R01CA136606 to XC; P30DK026743 for UCSF Liver Center; grant from the Deutsche Forschungsgemeinschaft DFG (grant number Ev168/2-1) to ME

List of Abbreviations

4EBP1	eukaryotic translation initiation factor 4E-binding protein 1
AK1	adenylate kinase 1
AKT	v-akt murine thymoma viral oncogene homolog
CMKP1	cytidine monophosphate kinase 1
ENTPD5	ectonucleoside triphosphate diphosphohydrolase 5
HCC	hepatocellular carcinoma
eIF4E	eukaryotic translation initiation factor 4E
MAPK	mitogen-activated protein kinase
mTOR	mammalian target of rapamycin
mTORC1	mTOR complex 1
N-Ras	neuroblastoma Ras viral oncogene homolog
Raptor	regulatory-associated protein of mTOR
RPS6	ribosomal protein S6
TFAM	mitochondrial transcription factor A

References

1. Parkin DM, Bray F, Ferlay J, Pisani P. Global cancer statistics, 2002. CA Cancer J Clin. 2005; 55:74–108. [PubMed: 15761078]
2. Bruix J, Sherman M. Management of hepatocellular carcinoma. Hepatology. 2005; 42:1208–1236. [PubMed: 16250051]
3. Bruix J, Sherman M. Management of hepatocellular carcinoma: an update. Hepatology. 2011; 53:1020–1022. [PubMed: 21374666]
4. El-Serag HB. Hepatocellular carcinoma. N Engl J Med. 2011; 365:1118–1127. [PubMed: 21992124]

5. Llovet JM, Ricci S, Mazzaferro V, Hilgard P, Gane E, Blanc JF, de Oliveira AC, et al. Sorafenib in advanced hepatocellular carcinoma. N Engl J Med. 2008; 359:378–390. [PubMed: 18650514]
6. Llovet JM, Bruix J. Molecular targeted therapies in hepatocellular carcinoma. Hepatology. 2008; 48:1312–1327. [PubMed: 18821591]
7. Villanueva A, Llovet JM. Targeted therapies for hepatocellular carcinoma. Gastroenterology. 2011; 140:1410–1426. [PubMed: 21406195]
8. Whittaker S, Marais R, Zhu AX. The role of signaling pathways in the development and treatment of hepatocellular carcinoma. Oncogene. 2010; 29:4989–5005. [PubMed: 20639898]
9. Yuan TL, Cantley LC. PI3K pathway alterations in cancer: variations on a theme. Oncogene. 2008; 27:5497–5510. [PubMed: 18794884]
10. Manning BD, Cantley LC. AKT/PKB signaling: navigating downstream. Cell. 2007; 129:1261–1274. [PubMed: 17604717]
11. Calvisi DF, Wang C, Ho C, Ladu S, Lee SA, Mattu S, Destefanis G, et al. Increased lipogenesis, induced by AKT-mTORC1-RPS6 signaling, promotes development of human hepatocellular carcinoma. Gastroenterology. 2011; 140:1071–1083. [PubMed: 21147110]
12. Zoncu R, Efeyan A, Sabatini DM. mTOR: from growth signal integration to cancer, diabetes and ageing. Nat Rev Mol Cell Biol. 2011; 12:21–35. [PubMed: 21157483]
13. Villanueva A, Chiang DY, Newell P, Peix J, Thung S, Alsinet C, Tovar V, et al. Pivotal role of mTOR signaling in hepatocellular carcinoma. Gastroenterology. 2008; 135:1972–1983. 1983 e1971-1911. [PubMed: 18929564]
14. Sengupta S, Peterson TR, Laplante M, Oh S, Sabatini DM. mTORC1 controls fasting-induced ketogenesis and its modulation by ageing. Nature. 2010; 468:1100–1104. [PubMed: 21179166]
15. Menon S, Yecies JL, Zhang HH, Howell JJ, Nicholatos J, Harputlugil E, Bronson RT, et al. Chronic activation of mTOR complex 1 is sufficient to cause hepatocellular carcinoma in mice. Sci Signal. 2012; 5:ra24. [PubMed: 22457330]
16. Laplante M, Sabatini DM. mTOR Signaling in Growth Control and Disease. Cell. 2012; 149:274–293. [PubMed: 22500797]
17. Hung CM, Garcia-Haro L, Sparks CA, Guertin DA. mTOR-Dependent Cell Survival Mechanisms. Cold Spring Harb Perspect Biol. 2012
18. Hsieh AC, Costa M, Zollo O, Davis C, Feldman ME, Testa JR, Meyuhas O, et al. Genetic dissection of the oncogenic mTOR pathway reveals druggable addiction to translational control via 4EBP-eIF4E. Cancer Cell. 2010; 17:249–261. [PubMed: 20227039]
19. Dowling RJ, Topisirovic I, Alain T, Bidinosti M, Fonseca BD, Petroulakis E, Wang X, et al. mTORC1-mediated cell proliferation, but not cell growth, controlled by the 4E-BPs. Science. 2010; 328:1172–1176. [PubMed: 20508131]
20. She QB, Halilovic E, Ye Q, Zhen W, Shirasawa S, Sasazuki T, Solit DB, et al. 4E-BP1 is a key effector of the oncogenic activation of the AKT and ERK signaling pathways that integrates their function in tumors. Cancer Cell. 2010; 18:39–51. [PubMed: 20609351]
21. Magnuson B, Ekim B, Fingar DC. Regulation and function of ribosomal protein S6 kinase (S6K) within mTOR signalling networks. Biochem J. 2012; 441:1–21. [PubMed: 22168436]
22. Volarevic S, Stewart MJ, Ledermann B, Zilberman F, Terracciano L, Montini E, Grompe M, et al. Proliferation, but not growth, blocked by conditional deletion of 40S ribosomal protein S6. Science. 2000; 288:2045–2047. [PubMed: 10856218]
23. Fumagalli S, Di Cara A, Neb-Gulati A, Natt F, Schwemberger S, Hall J, Babcock GF, et al. Absence of nucleolar disruption after impairment of 40S ribosome biogenesis reveals an rpL11-translation-dependent mechanism of p53 induction. Nat Cell Biol. 2009; 11:501–508. [PubMed: 19287375]
24. Ruvinsky I, Sharon N, Lerer T, Cohen H, Stolovich-Rain M, Nir T, Dor Y, et al. Ribosomal protein S6 phosphorylation is a determinant of cell size and glucose homeostasis. Genes Dev. 2005; 19:2199–2211. [PubMed: 16166381]
25. Guertin DA, Sabatini DM. The pharmacology of mTOR inhibition. Sci Signal. 2009; 2:pe24. [PubMed: 19383975]

26. Wander SA, Hennessy BT, Slingerland JM. Next-generation mTOR inhibitors in clinical oncology: how pathway complexity informs therapeutic strategy. J Clin Invest. 2011; 121:1231–1241. [PubMed: 21490404]
27. Choo AY, Yoon SO, Kim SG, Roux PP, Blenis J. Rapamycin differentially inhibits S6Ks and 4E-BP1 to mediate cell-type-specific repression of mRNA translation. Proc Natl Acad Sci U S A. 2008; 105:17414–17419. [PubMed: 18955708]
28. Choo AY, Blenis J. Not all substrates are treated equally: implications for mTOR, rapamycinresistance and cancer therapy. Cell Cycle. 2009; 8:567–572. [PubMed: 19197153]
29. Calvisi DF, Ladu S, Gorden A, Farina M, Conner EA, Lee JS, Factor VM, et al. Ubiquitous activation of Ras and Jak/Stat pathways in human HCC. Gastroenterology. 2006; 130:1117–1128. [PubMed: 16618406]
30. Ho C, Wang C, Mattu S, Destefanis G, Ladu S, Delogu S, Armbruster J, et al. AKT and N-Ras coactivation in the mouse liver promotes rapid carcinogenesis by way of mTOR, FOXM1/SKP2, and c-Myc pathways. Hepatology. 2012; 55:833–845. [PubMed: 21993994]
31. Carlson CM, Frandsen JL, Kirchhof N, McIvor RS, Largaespada DA. Somatic integration of an oncogene-harboring Sleeping Beauty transposon models liver tumor development in the mouse. Proc Natl Acad Sci U S A. 2005; 102:17059–17064. [PubMed: 16286660]
32. Chen X, Calvisi DF. Hydrodynamic Transfection for Generation of Novel Mouse Models for Liver Cancer Research. Am J Pathol. 2014; 184:912–923. [PubMed: 24480331]
33. Srinivas S, Watanabe T, Lin CS, William CM, Tanabe Y, Jessell TM, Costantini F. Cre reporter strains produced by targeted insertion of EYFP and ECFP into the ROSA26 locus. BMC Dev Biol. 2001; 1:4. [PubMed: 11299042]
34. Wang C, Cigliano A, Delogu S, Armbruster J, Dombrowski F, Evert M, Chen X, et al. Functional crosstalk between AKT/mTOR and Ras/MAPK pathways in hepatocarcinogenesis: implications for the treatment of human liver cancer. Cell Cycle. 2013; 12:1999–2010. [PubMed: 23759595]
35. Ruggero D. Translational control in cancer etiology. Cold Spring Harb Perspect Biol. 2013; 5
36. Fang M, Shen Z, Huang S, Zhao L, Chen S, Mak TW, Wang X. The ER UDPase ENTPD5 promotes protein N-glycosylation, the Warburg effect, and proliferation in the PTEN pathway. Cell. 2010; 143:711–724. [PubMed: 21074248]
37. Shen Z, Huang S, Fang M, Wang X. ENTPD5, an endoplasmic reticulum UDPase, alleviates ER stress induced by protein overloading in AKT-activated cancer cells. Cold Spring Harb Symp Quant Biol. 2011; 76:217–223. [PubMed: 22169232]
38. Morita M, Gravel SP, Chenard V, Sikstrom K, Zheng L, Alain T, Gandin V, et al. mTORC1 controls mitochondrial activity and biogenesis through 4E-BP-dependent translational regulation. Cell Metab. 2013; 18:698–711. [PubMed: 24206664]
39. Carroll M, Borden KL. The oncogene eIF4E: using biochemical insights to target cancer. J Interferon Cytokine Res. 2013; 33:227–238. [PubMed: 23472659]
40. Lee T, Pelletier J. Eukaryotic initiation factor 4F: a vulnerability of tumor cells. Future Med Chem. 2012; 4:19–31. [PubMed: 22168162]
41. Wang XL, Cai HP, Ge JH, Su XF. Detection of eukaryotic translation initiation factor 4E and its clinical significance in hepatocellular carcinoma. World J Gastroenterol. 2012; 18:2540–2544. [PubMed: 22654452]
42. Buitrago-Molina LE, Pothiraju D, Lamlé J, Marhenke S, Kossatz U, Breuhahn K, Manns MP, et al. Rapamycin delays tumor development in murine livers by inhibiting proliferation of hepatocytes with DNA damage. Hepatology. 2009; 50:500–509. [PubMed: 19642171]
43. Cencic R, Desforges M, Hall DR, Kozakov D, Du Y, Min J, Dingledine R, et al. Blocking eIF4E–eIF4G interaction as a strategy to impair coronavirus replication. J Virol. 2011; 85:6381–6389. [PubMed: 21507972]
44. Martineau Y, Azar R, Muller D, Lasfargues C, El Khawand S, Anesia R, Pelletier J, et al. Pancreatic tumours escape from translational control through 4E-BP1 loss. Oncogene. 2014; 33:1367–1374. [PubMed: 23563181]

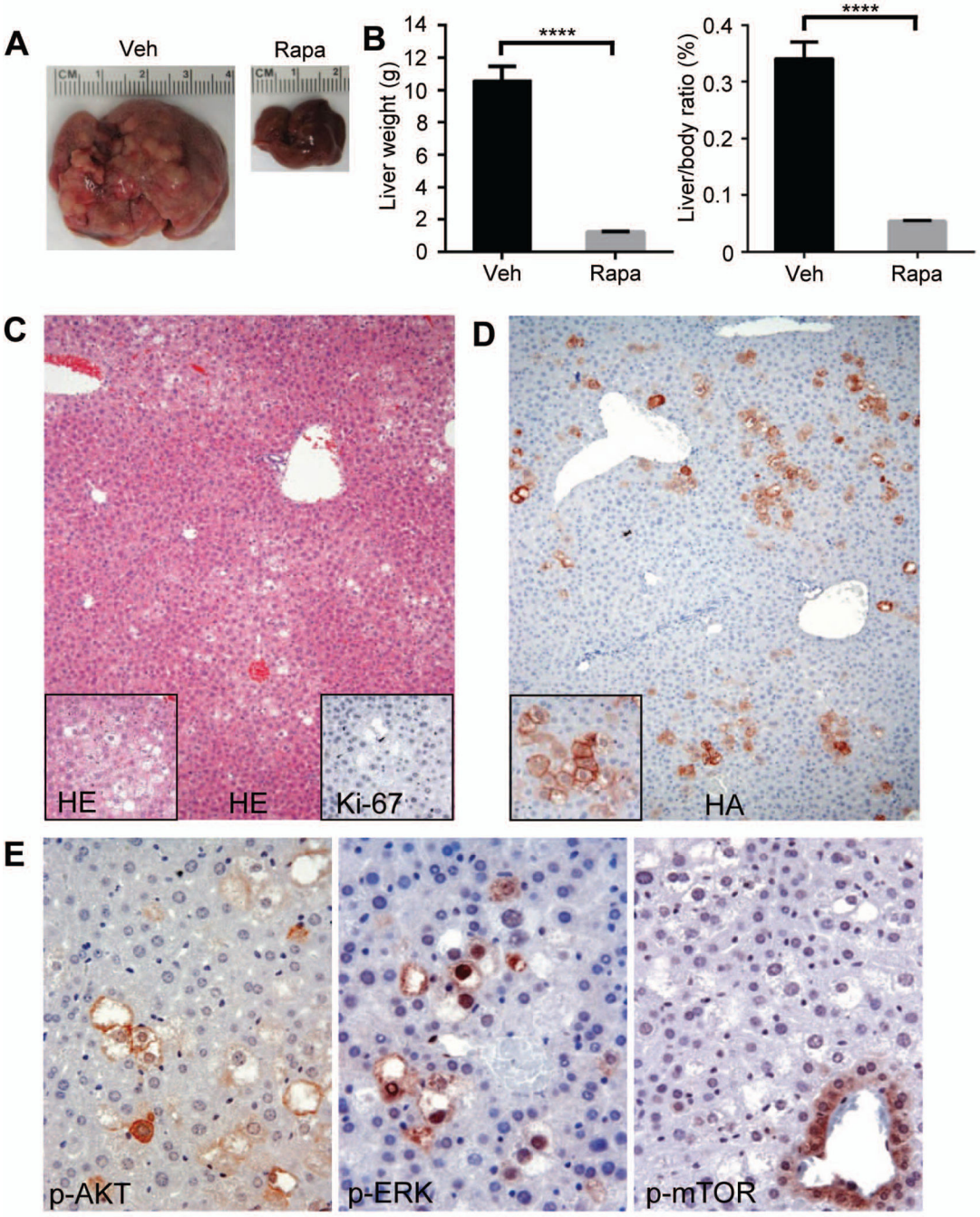

Fig. 1.

Rapamycin treatment effectively inhibits AKT/Ras induced hepatocarcinogenesis. (A) Gross images of livers, (B) liver weight and liver to body weight ratio of AKT/Ras mice treated with vehicle (Veh) or Rapamycin (Rapa) for 7 weeks. Data are presented as mean ± SEM. ****P<0.0001. (C) Hematoxylin & eosin (HE) and Ki67, (D) HA-tag, (E) p-AKT, p-ERK and p-mTOR staining in Rapamycin treated ATK/Ras mouse liver tissues. Magnifications: 100× (C&D); 400× (E and insets). 148×190mm (300 × 300 DPI)

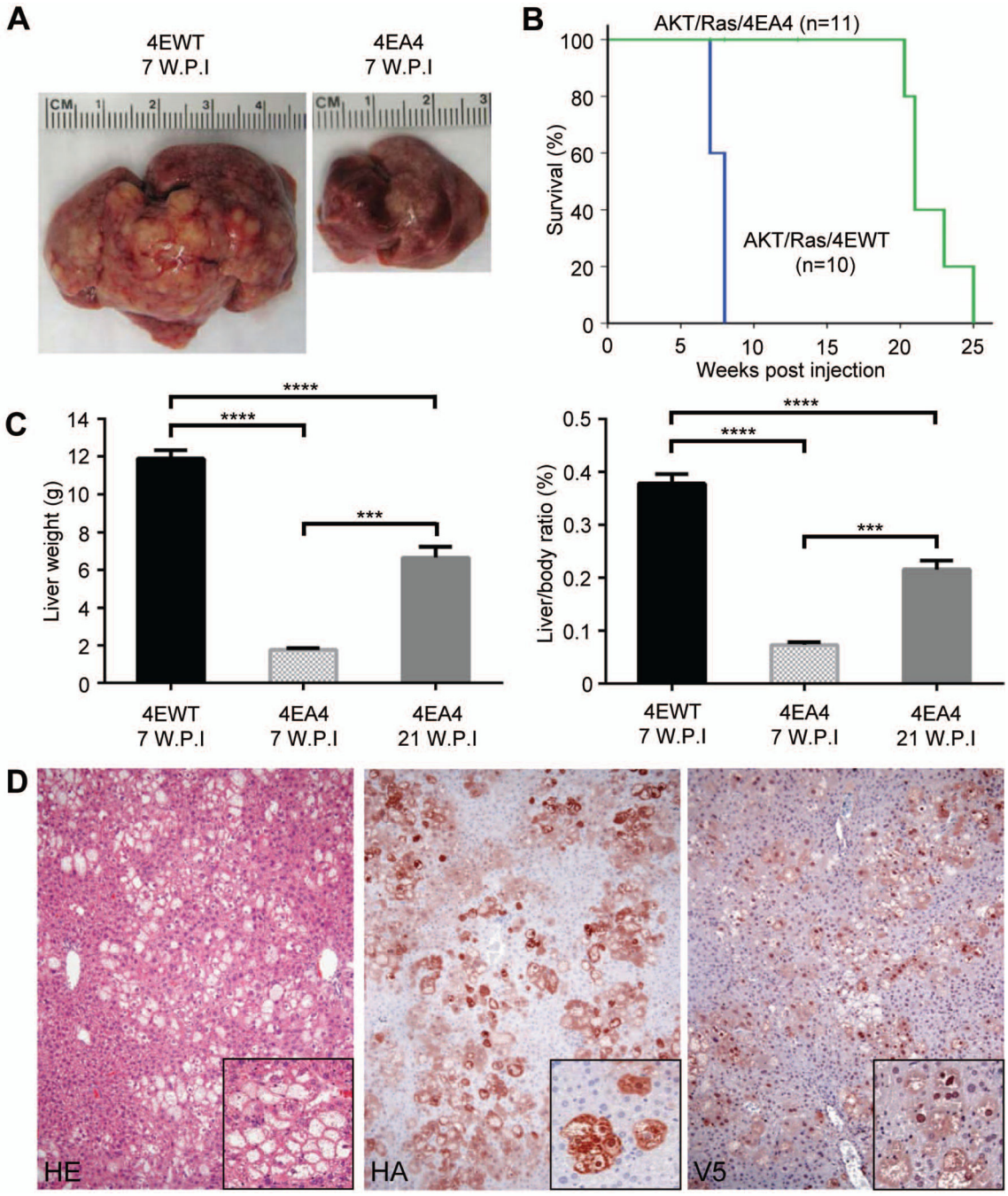

Fig. 2.

4EBP1A4 effectively delays AKT/Ras induced hepatocarcinogenesis. (A) Gross images of livers, (B) survival curve, (C) liver weight and liver to body weight ratio of AKT/Ras/4EBP1WT (4EWT) and AKT/Ras/4EBP1A4 (4EA4) injected mice at different time points. Data are presented as mean ± SEM. ***P<0.001; ****P<0.0001. (D) HE image, HA-AKT, V5-4EBP1A4 staining in AKT/Ras/4EBP1A4 injected mouse liver 7 weeks post injection (W.P.I.). Magnifications: 100×; 400× (insets). 160×197mm (300 × 300 DPI)

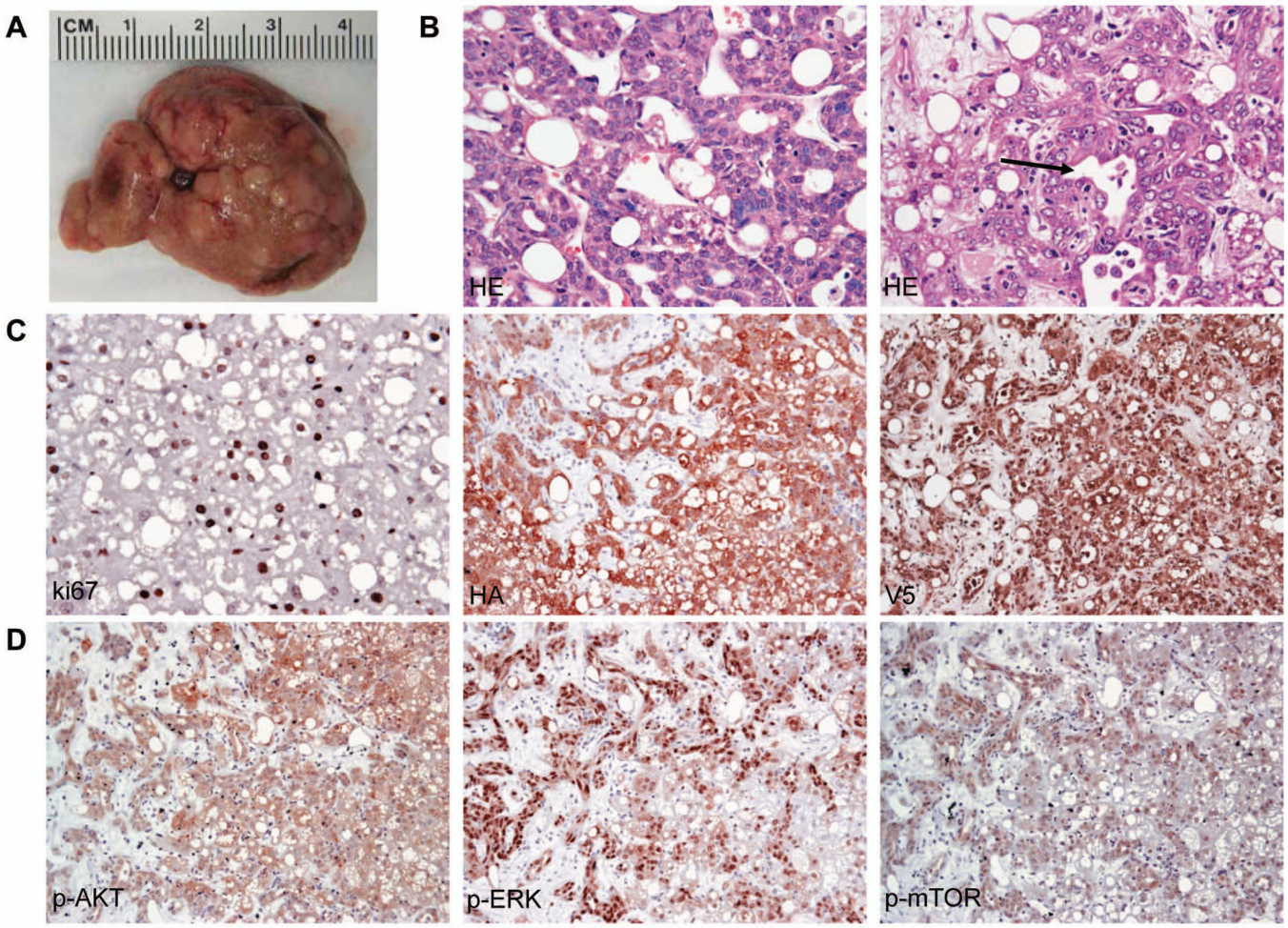

Fig. 3.

AKT/Ras induces liver tumor formation in the presence of 4EBP1A4 after long latency. (A) Gross images of AKT/Ras/4EBP1A4 injected mouse livers 21 W.P.I. (B) HE images of a small hepatocellular carcinoma (left) and a mixed hepatocellular-cholangiocellular tumor (right, arrow indicates ductular features), (C) Ki-67, HA-AKT, V5-4EBP1A4, (D) p-AKT, p-ERK, and p-mTOR staining in the liver tumors developed in AKT/Ras/4EBP1A4 injected mice. Magnifications: 400× (HE and Ki67); 200× (HA, V5, p-AKT, p-ERK, p-mTOR). 220×168mm (300 × 300 DPI)

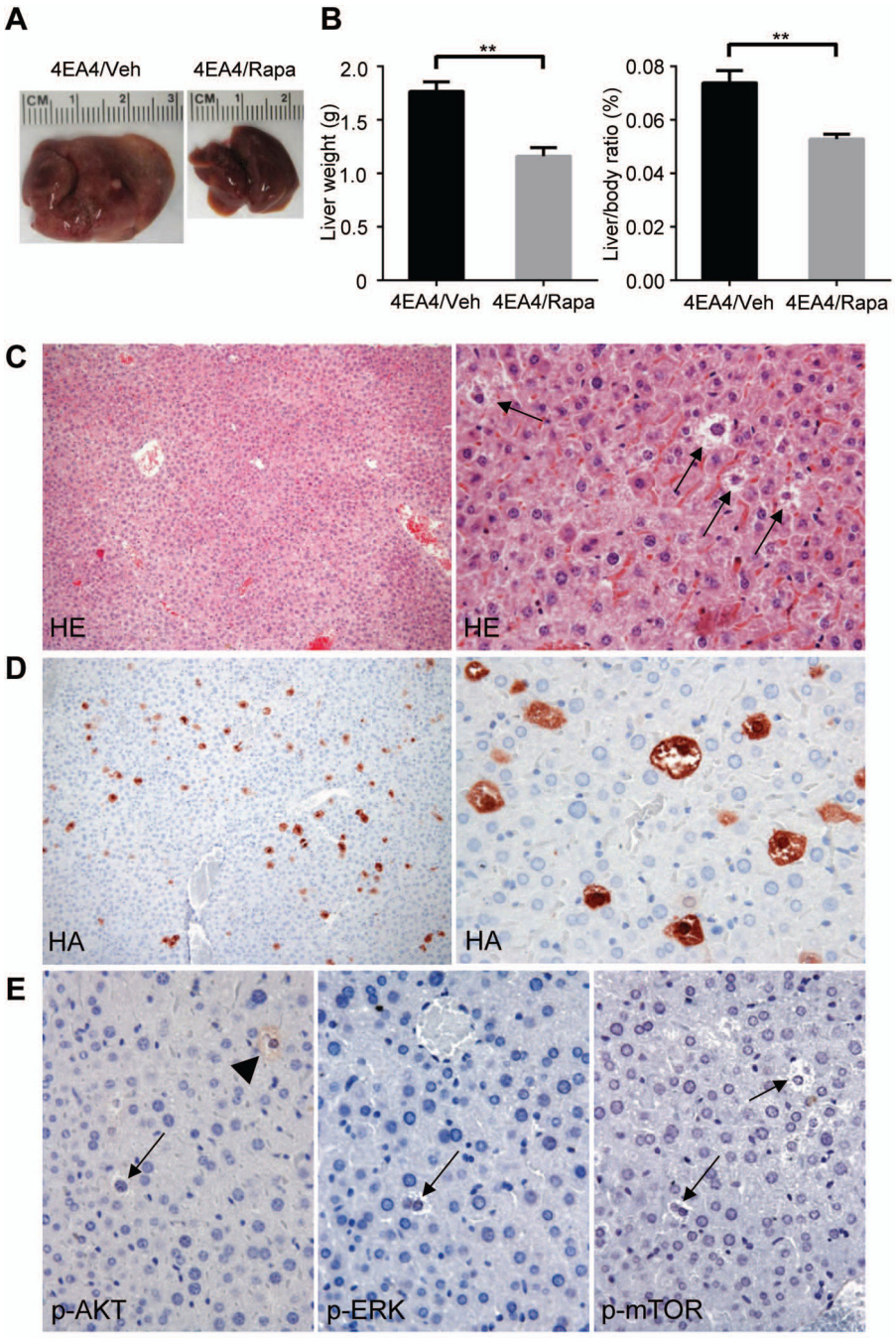

Fig. 4.

Combined Rapamycin treatment and 4E-BP1A4 transfection completely inhibits AKT/Ras-driven hepatocarcinogenesis. (A) Gross images of livers, (B) liver weight and liver to body weight ratio of AKT/Ras/4EBP1A4 mice treated with vehicle or Rapamycin for 7 weeks. Data are presented as mean ± SEM. **P<0.01. (C) HE images, (D) HA-AKT and (E) p-AKT, p-ERK, p-mTOR staining in Rapamycin-treated AKT/Ras/4EBP1A4 mouse liver. Arrows point to clear-cell hepatocytes. Arrowhead marks weak p-AKT staining in the cytoplasm of a clear-cell hepatocyte. Magnifications: 100× (low magnification of HE and

HA); 400× (high magnification of HE, HA, p-AKT; p-ERK, p-mTOR). 148×223mm (300 × 300 DPI)

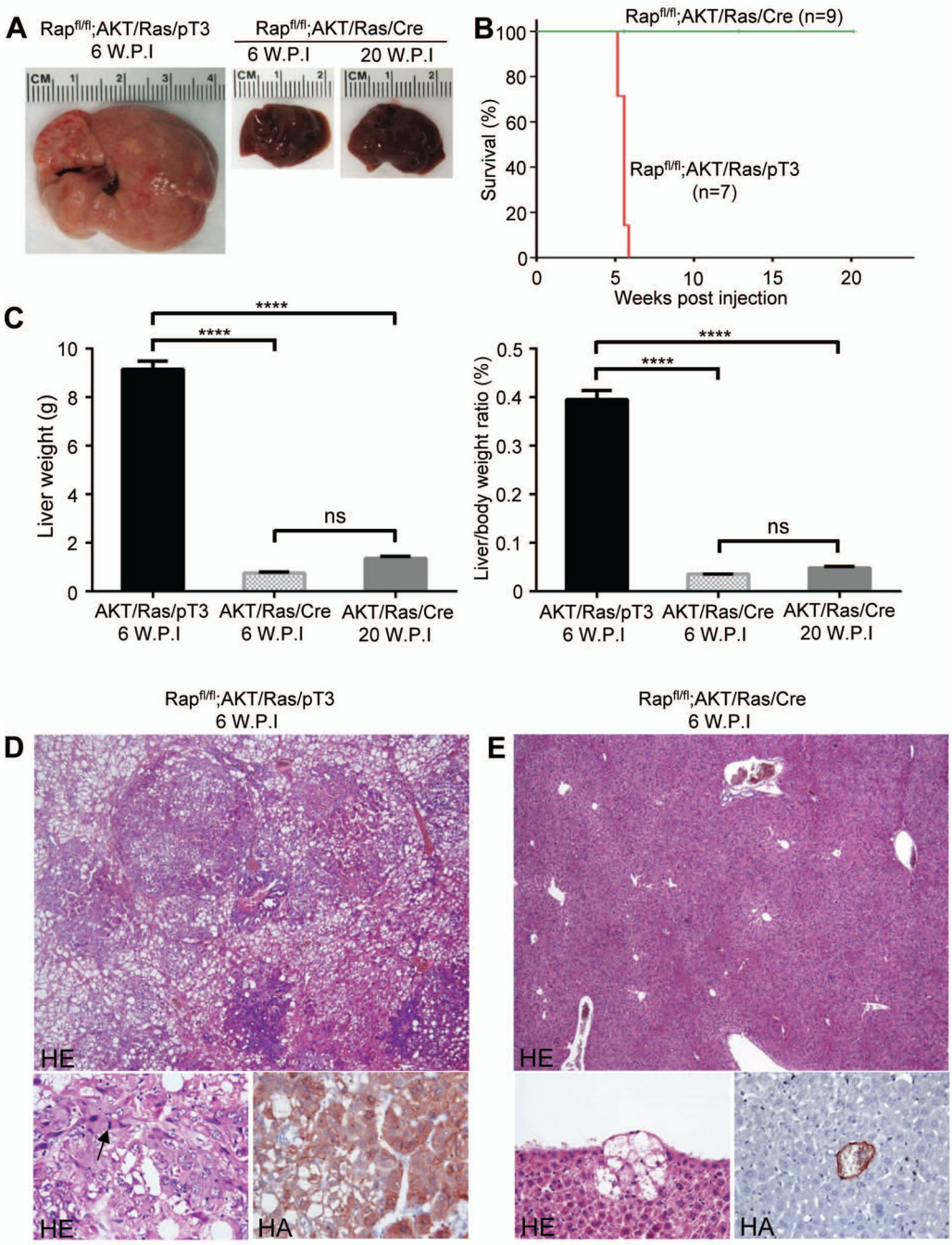

Fig. 5.

Ablation of Raptor completely inhibits AKT/Ras hepatocarcinogenesis. (A) Gross images of livers, (B) survival curve, (C) liver weight and liver to body weight ratio of AKT/Ras/pT3 or AKT/Ras/Cre injected Raptorfl/fl mice. Data are presented as mean ± SEM. ****P<0.0001; ns: not significant. (D) HE images and HA-AKT staining in AKT/Ras/pT3 injected Raptorfl/fl mouse liver. The arrow indicates a mitotic figure within an HCC. (E) HE image and HA-AKT staining in AKT/Ras/Cre injected Raptorfl/fl mice. Magnifications: 40× (upper panel); 400× (lower panel). 167×223mm (300 × 300 DPI)

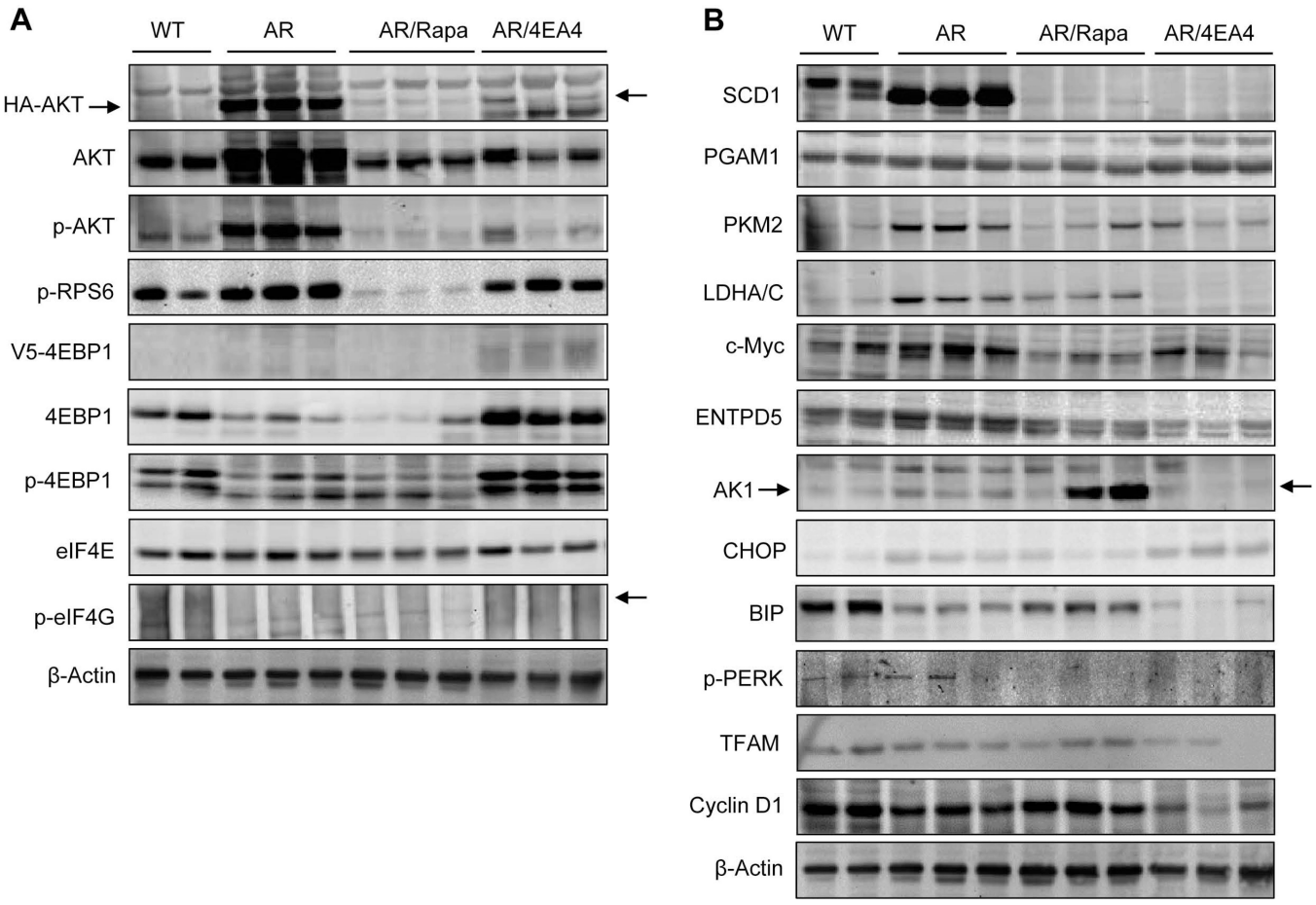

Fig. 6.

Representative immunoblotting in wild-type (WT), AKT/Ras (AR), AKT/Ras/Rapa (AR/Rapa) and AKT/Ras/4EBP1A4 (AR/4EA4) liver tissues. Five to 8 samples per group were used. Arrows at the left and right side of the blots indicate the correct band for these proteins. 213×158mm (300 × 300 DPI)

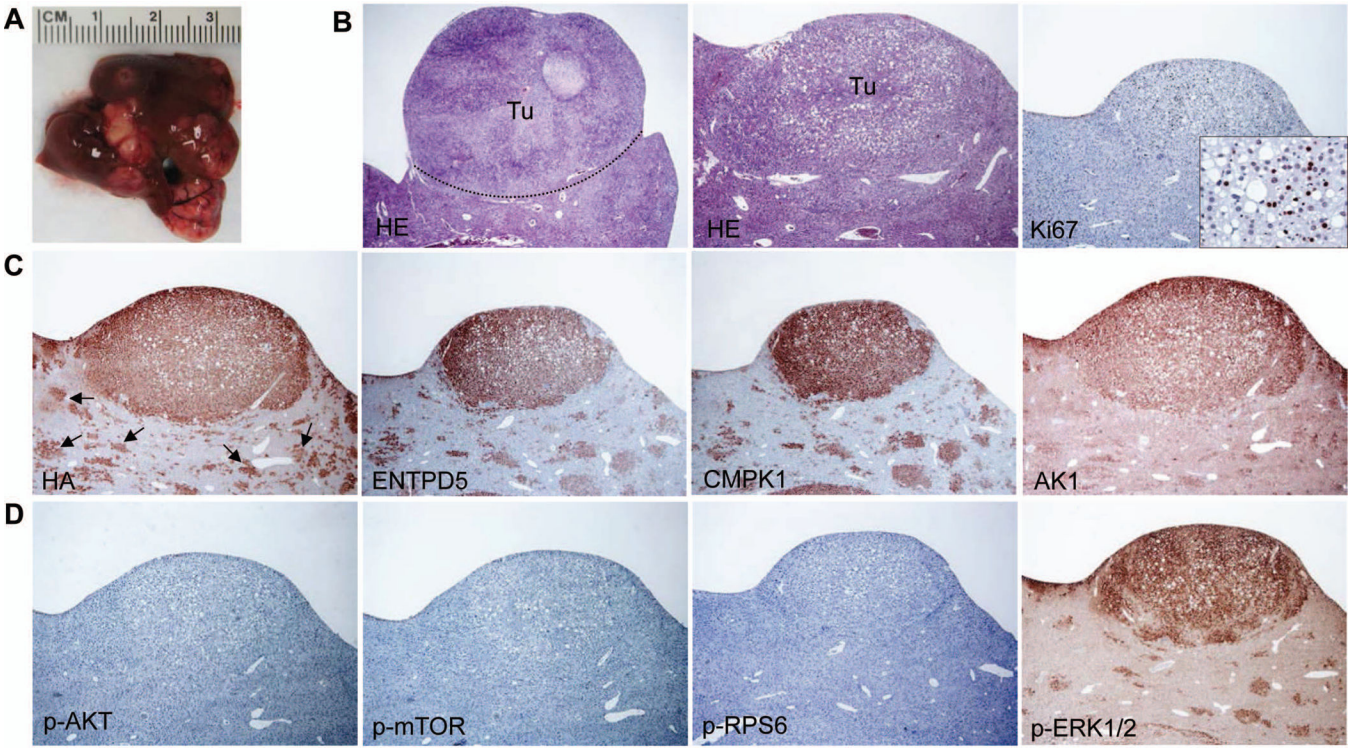

Fig. 7.

eIF4E and Ras co-expression in liver induces hepatocarcinogenesis in mice. (A) Macroscopic appearance of eIF4E/Ras-injected mouse liver 30 weeks after hydrodynamic injection. (B) HE image and Ki67 staining, (C) HA-eIF4E, ENTPD5, CMPK1, AK1, (D) p-AKT, p-mTOR, p-RPS6, and p-ERK1/2 staining in eIF4E/Ras-injected mouse liver 30 weeks after hydrodynamic. Tu: hepatocellular tumors; the dotted line marks the tumor area. Arrows indicate preneoplastic areas. Magnifications: 20× (first HE image in B); 40× (all remaining images); 400× (inset). 239×141mm (300 × 300 DPI)

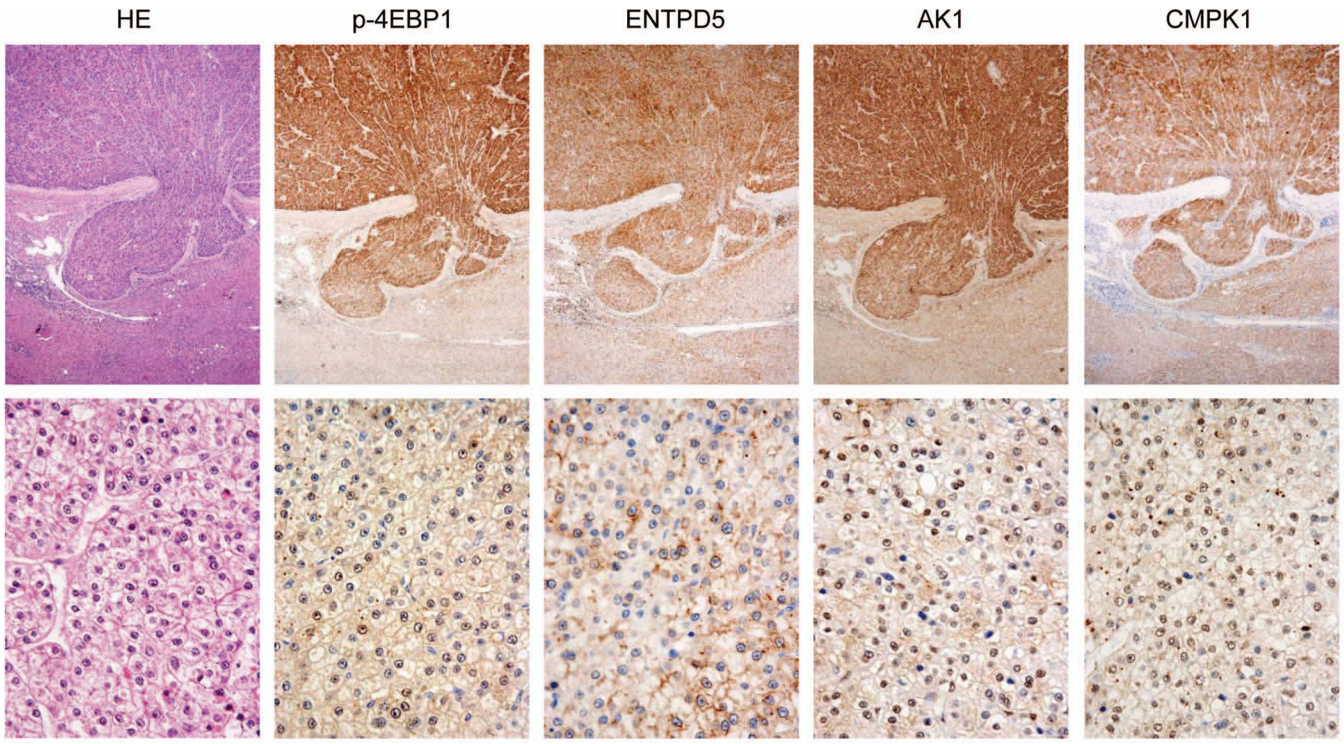

Fig. 8.

4EBP1 controls the expression of ENTPD5 and its targets in human hepatocellular carcinoma (HCC). Concomitant induction and co-localization of p-4EBP1, ENTPD5, AK1 and CMPK1 in an HCC (upper panel; magnification: 40×). Low levels of p-4EBP1, ENTPD5, AK1 and CMPK1 in another HCC (lower panel; magnification: 400×). 230×134mm (300 × 300 DPI)